

INVESTIGATION ON CALORIMETRIC AND ELASTIC PROPERTIES OF 50TeO₂-(50-x)V₂O₅-xK₂O GLASSY SYSTEMS

M. FARAHMANDJOU^{a*}, S. A. SALEHIZADEH^b

^a*Department of Physics, Varamin Pishva Branch, Islamic Azad University, Varamin, Iran*

^b*Department of Physics and I3N, University of Aveiro, Campus Santiago, 3810-193 Aveiro, Portugal*

In this work, the thermal behavior of ternary glassy compositions of 50TeO₂-(50-x)V₂O₅-xK₂O compositions with $0 \leq x \leq 20$ (in mol%) prepared using the press-melt quenching method has been investigated. By utilizing Makishima and Makenzie's theory, some elastic features such as Young's modulus, bulk modulus, and shear modulus were calculated indicating a strong relation between elastic properties and structure of glass. In addition, the heating rate dependence of T_g was investigated using different theoretical models describing the glass transition. The activation energy values (ΔH^*) for 50TVK0, 50TVK5 and 50TVK10 at different heating-rate regions were obtained, using Kissinger and Moynihan models. The results from both models showed two different values for the activation energy in each heating rate region suggesting strong heating rate dependency of activation energy process. Furthermore the observed similarity in ΔH^* values for both models suggests that both equations are useful in determining ΔH^* . The fragility parameter ($m = \Delta H^*/R.T_g$) was calculated for the samples. The results shows 50TVK10 have the lowest fragility, 17.58, indicating this composition can be considered as strong glass with good resistance against thermal shocks. Also a logical correlation was found between kinetic fragility parameter and elastic modulus confirming agreement between experimental and theoretical results. The obtained data was studied in order to indicate of the influence of addition of K₂O as network modifier on thermal stability, glass-forming tendency and fragility.

(Received September 26, 2015; Accepted November 20, 2015)

Keywords: Amorphous Materials, Differential Scanning Calorimetry, Glass Transition Temperature, Fragility and Shear Modulus

1. Introduction

There are lot of scope for investigation of tellurium oxide based glasses rather than borate and silicate glasses as a result of their considerable physical properties like high glass forming ability, no hygroscopic properties, high thermal expansion coefficients, low glass transition (T_g), low melting-point, large third-order non-linear susceptibility, high refractive index and high infrared transmission, low melting temperature and high dielectric constant [1-13].

Addition of such as alkali, alkaline earth and transitional metal oxides (TMO) or other as a network modifier or intermediate oxide network to tellurite base glasses can lead to enhance the chemical stability and devitrification of compositions providing numerous technological applications in industry[14-15]. The TeO₂-V₂O₅ amorphous systems possess semiconducting behavior which is attributed from that vanadium ions have two valence states and the electrical conductivity is raised from electrons hopping between V⁴⁺ and V⁵⁺ ions sites [4, 15 and 16].

Furthermore, the influence of mixing alkali oxides, M₂O, (where M= Li, Na, K, Rb or Cs) to TeO₂ based glasses can be seen in term with several characteristics including viscosity,

* Corresponding author: farahmandjou@iauvaramin.ac.ir

chemical durability, electrical conductivity, mechanical relaxation and glass forming tendency because of the production of non-bridging oxygen (NBO) sites which decrease the average coordination number, thus resulting in the resistant glasses to crystallization [17-19].

Study in the DSC spectra of the compositions is a conventional method to interpret the thermal properties of glasses which are suitable for optical applications. The important point in ideal laser materials is that they should bear high thermal loads and thus will be subjected to crystallization during laser operation [1]. The activation energy of the glass transition, ΔH^* , is one key parameter showing the dependence of T_g on heating rate which determines different mechanisms involved in the transition process [20]. Furthermore, the strength of glasses can be identified with changes in heat capacity in the glass transition region. The fragile glasses such as iron phosphate and Chalcogenide have ionic or molecular network with a non-Arrhenian behavior in the temperature dependence of viscosity. While for a strong glass possessing covalent network, one can see linearity in the $\log \eta$ versus $1/T$ plot [20].

On other side, the variation in the stoichiometry of the multicomponent glassy systems has a significant impact on the mechanical and elastic properties such as microhardness, Poisson ratio, packing density and elastic modulus which can be helpful to find ideal composition satisfying high thermal stability against thermal shocks for practical applications.

To the best of our knowledge on the calorimetric and elastic properties of the tricomponent $\text{TeO}_2\text{-V}_2\text{O}_5\text{-A}_n\text{O}_m$ which AnO_m is another oxide including CuO [21], Fe_2O_3 [22], Ag_2O [23], NiO [24-26] MoO_3 [27] and Sb_2O_3 [28, 29], have been investigated extensively, due to the importance of the tellurite-vanadate systems in industrial applications. We recently have been investigated in the optical band gap and the tailing states of $\text{TeO}_2\text{-V}_2\text{O}_5\text{-K}_2\text{O}$ glasses [30]. Traces of crystalline peaks were not detected in XRD patterns, in as-cast samples. Therefore, the glasses used in the present work have effectively an amorphous structure. In this work, thus, we are going to study ternary tellurite-vanadate glasses containing potassium oxide in order to 1) evaluate the influence of addition K_2O to glasses on their structural configuration, 2) investigate in the degree of fragility and thermal stability of the compositions 3) study the variation of the activation energy of the glass transition and 4) find logical correlation between thermal and structural characters and also application of Makishima and Mackenzie's theory.

2. Experimental Procedure

The samples in the ternary $(50)\text{TeO}_2\text{-(50-x)}\text{V}_2\text{O}_5\text{-(x)}\text{K}_2\text{O}$ system with $x = 0, 5, 10, 15$ and 20 prepared by well dry mixing of 16g batches of the TeO_2 (MERCK, 99.99% pure), V_2O_5 (MERCK, 99.99% pure) and K_2CO_3 (MERCK, 99.99% pure) starting materials (hereafter, termed as 50TVK0, 50TVK5, 50TVK10, 50TVK15, 50TVK20, respectively). V_2O_5 , TeO_2 . The appropriate amounts of reactants were weighted using a precise balance (Kern ALS 220-4) having an accuracy of 0.1 mg and grounded in an agate mortar. The mixtures were pre-heated in atmospheric conditions at 350°C for 45 min in order to dehydrate them and then melted in a porcelain crucible up to 800°C for 1 h, in an electric furnace (ATBIN ALF 15) in air, the melts were stirred every 5 min to prevent the separation of the three components and also to remove CO_2 . Such obtained melts were poured on to a polished steel mould and immediately pressed by another polished steel block (press-melt quenching method), where the blocks were kept at room temperature. The amorphous character of the pellets was checked by X-ray diffraction using a Burker diffractometer (AXS D8 Advance) radiation CuK_α . The density (ρ) of each sample was calculated by Archimedes's method using para-xylene as an immersion liquid. The Calorimetric studies of each sample were done using Differential Scanning Calorimeter (DSC: Pyris1, USA) under dynamic N_2 gas atmosphere (at a constant rate of $20\text{ cm}^3/\text{min}$); also for each DSC measurement, the heating rates (ϕ) of 12, 15, 18 and 20 K/min were used to obtain the DSC curves. Vickers micro-hardness measurements were performed on samples in pellet form using a Beco 550x micro-hardness tester. All glass samples were uniformly subjected a load of 300 g for a 10 s duration at room temperature.

3. Result and discussion

3.1 Poisson ratio, Elastic characteristics and Microhardness

In the crystalline oxides the young's modulus is given by

$$E = \frac{2\alpha U}{r_o^3} \quad (1)$$

Which α is the madelung constant, U is electrostatic energy and r_o is the interatomic distance. While in glassy materials due to disorder in their structures, the madelung constant cannot be defined as for crystalline oxides [31].

According to the Makishima and Mackenzie's approach, we introduce the packing factor of oxide M_xO_y (V_i) and the packing density of multicomponent glass V_t , as the following:

$$V_i = \frac{4}{3} \pi N_A (x.R_M^3 + y.R_O^3) \quad (2)$$

$$V_t = V_M^{-1} \sum (x_i.V_i) \quad (3)$$

where R_M and R_O are the respective Pauling's ionic radius of metal M and oxygen O , N_A is Avogadro's number, V_M the molar volume of glass and x_i the mole fraction of oxide component i ; the values of V_M have been taken from our previous paper. Therefore, the Young's modulus E of oxide glasses can be expressed in term of the packing density of glass V_t and the dissociation energy per unit volume G_t , as:

$$E = 2V_t.G_t \quad (4)$$

Which G_t is calculated using the equation as:

$$G_t = \sum (x_i.G_i) \quad (5)$$

Where G_i is dissociation energy per unit volume of the i th oxide.

So, now we can deduce some elastic parameters such as bulk modulus and shear modulus as the following [31]:

$$E = 1.2V_t.K, E = 2.4 V_t.G_t^2 \quad (6)$$

$$S = \frac{3EK}{(9K - E)} \quad (7)$$

The obtained data has been listed in table1. In the calculation, the dissociation energy corresponding to each oxide has been brought from [32, 33].

On other side, the poisson ratio is the quotient of the transverse strain and the axial strain of a solid under a uniaxial stress, and the lateral strain would be smaller in loosely packed glasses because there is more space for the atomic movement [24]. In other word, the Poisson ratio in the loosely packed oxide glass is small while for the glasses where atoms are tightly packed in, we have higher Poisson ratio values. According to the Makishima and Mackenzie model, Poisson ratio can be theoretically deduced as:

$$\mu_{\text{cal}} = 0.5 - \frac{1}{7.2V_t} \quad (8)$$

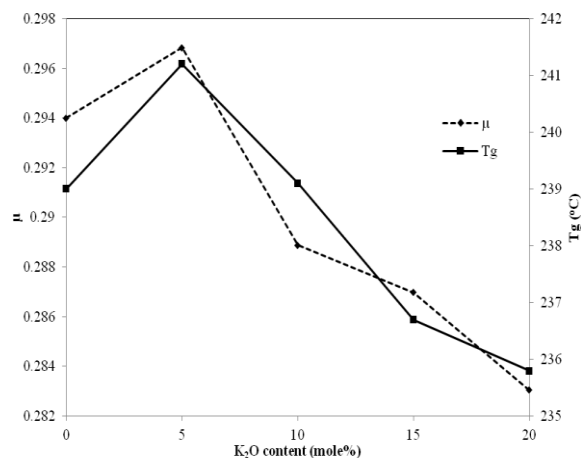


Fig. 1. Variations of glass transition temperature and Poisson's ratio for 50TVKx glasses

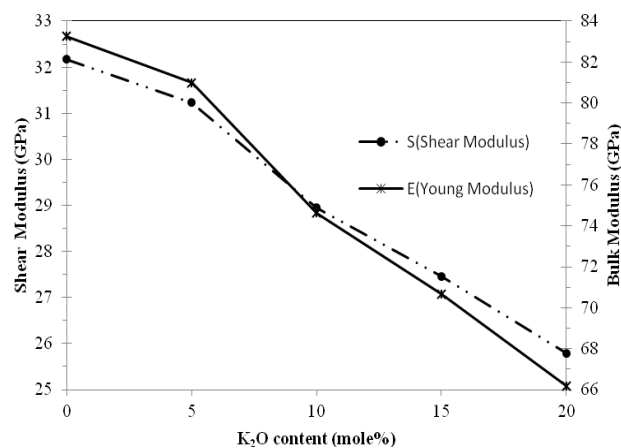


Fig. 2. Bulk modulus and Shear modulus versus K₂O content in 50TVKx glasses.

According to fig. 1 Results show that at low addition K₂O, Poisson ratio increases to 0.297 whereas when Potassium concentration up to 20% mol one can see a slight reduction in μ to 0.283 for the glassy systems which is similar to the observed behavior in the T_g values of the compositions.

In comparison with other works related with the elastic properties of the tellurite-vanadate glasses containing Ag₂O [35] and Sb₂O₃ [28], it can be seen that addition of silver oxide and antimony oxide to tellurite - vanadate systems leads to decreasing in Shear, Bulk and Young's modulus as same as behavior for the understudied glasses, 50TeO₂-(50-x)V₂O₅-xK₂O, as illustrated from table 1 and fig. 2 and 3. However, elastic moduli of the present glasses in average are higher than that of TeO₂-V₂O₅-Ag₂O and TeO₂-V₂O₅-Sb₂O₃ glasses, introducing tellurite-vanadate-potassium glassy systems are more suitable for technological applications. Furthermore, insertion of the glass modifier K₂O up to 20 mol % will cause to smooth decreasing in both shear and Young's modulus from 83.263 and 30.322 Gpa to 66.181 and 25.790 GPa, respectively. The descending trend of the elastic moduli of the compositions can be attributed to the decrease in the average number of bonds per unit volume in the samples. It is obvious from the obtained results that the type of bonding in the network structure plays a dominant role in deciding the rigidity of

these glass structures. It is believed that the behavior of both shear and Young's moduli are associated with the change in cross-linkage and coordination of the glass network [36].

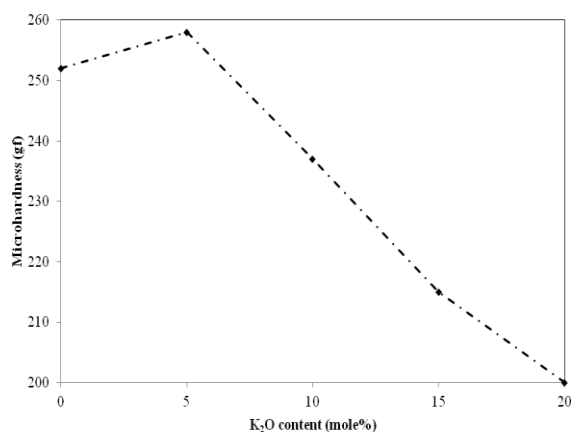


Fig. 3. Microhardness versus K_2O content in 50TVKx glasses.

As seen in fig.3, the microhardness of the compositions reaches to a maximum in 50TVK5 glass and then it decreases drastically to 200 Kgmm^{-2} in 50TVK20 system. This trend is almost close to the density variation in respect with K_2O content which can be related to the different bond energy in K–O and V–O. When V_2O_5 is substituted by K_2O . The variation of microhardness as a function of vanadium content in the binary and ternary TeO_2 - V_2O_5 glasses can be attributed to the softness and $[V^{5+}/V^{4+}]$ ratio [37]. This data shows an interesting similarity with the results obtained from T_g and poisson ratio.

Table 1. Values of density ρ [30], glass transition temperature T_g , molar volume V_m , Poisson's ratio (μ), Young's modulus E , bulk modulus K and shear modulus S for 50TVKx glasses

Glass	x (mol%)	ρ ($gr.cm^{-3}$)	V_m (cm^3/mol)	T_g ($^{\circ}C$) in $\varphi=12^{\circ}C/min$	Microhardness ($Kgmm^{-2}$)	μ ($\pm 1\%$)	E (GPa) ($\pm 1\%$)	S (GPa) ($\pm 1\%$)	K (GPa) ($\pm 1\%$)
50TVK0	0	4.577 \pm 0.002	37.304	239 \pm 0.1	252 \pm 7	0.294	83.263	32.173	67.362
50TVK5	5	4.678 \pm 0.004	35.561	241.2 \pm 0.1	258 \pm 9	0.297	80.987	31.225	66.436
50TVK10	10	4.540 \pm 0.005	35.677	239.1 \pm 0.1	237 \pm 10	0.289	74.627	28.950	58.912
50TVK15	15	4.526 \pm 0.004	34.710	236.7 \pm 0.1	215 \pm 6	0.287	70.680	27.460	55.297
50TVK20	20	4.501 \pm 0.003	34.038	235.8 \pm 0.1	200 \pm 2	0.283	66.181	25.790	50.840

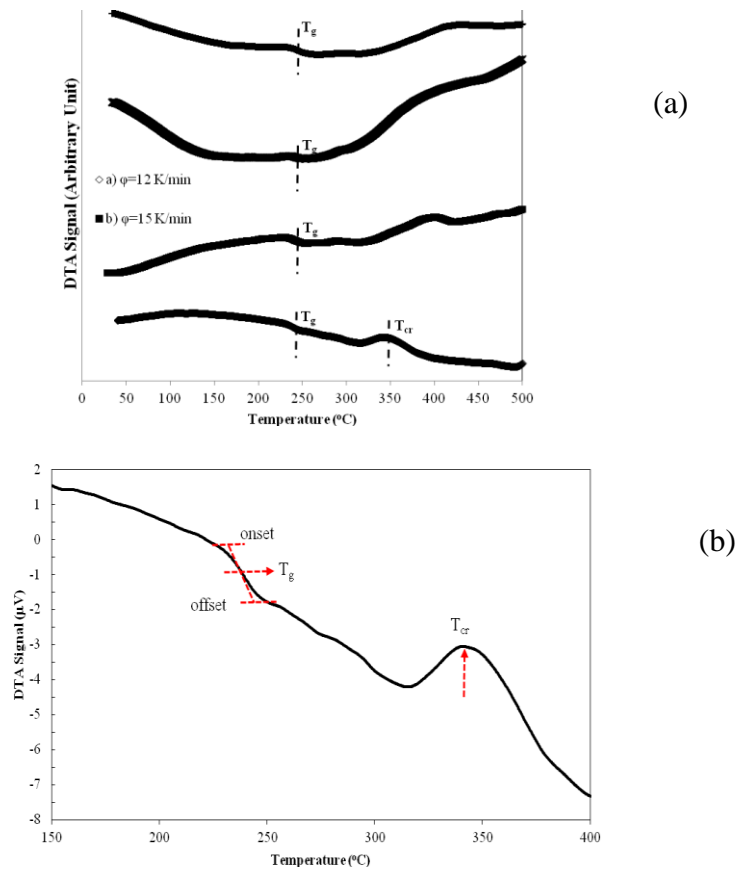


Fig. 4. a) DSC curves in 50TVK0 glass in different heating rates: a) $\phi=12$ K/min, b) $\phi=15$ K/min, c) $\phi=18$ K/min and d) $\phi=20$ K/min. b) A typical heating flow vs. temperature curve for a 50TeO₂-50V₂O₅, mol%, glass at a heating rate of 12 K/min

Fig. 4 a shows typical non-isothermal DSC curves for 50TVK0 in different heating rates ($\phi=12, 15, 18$ and 20 K/min). The characteristic phenomena, glass transition region and crystallization process are evident in the DSC thermograms in the temperature range of investigation as shown with more clarity in fig 4 b. As a descriptive analysis, the DSC thermogram is divided into two parts: 1) the presence of an endothermic peak, marked on the baseline, indicates the occurrence of a heat-absorbing event such as glass transition or melting, while 2) the exothermic peak is related to the crystallization which occurs as a result of some sort of heat-releasing event. The glass transition temperature T_g indicates a change of viscosity which is not essentially Arrhenius, representing the strength or rigidity of the glassy structure of the alloy as an amorphous solid transform to a super cooled liquid state [38]. It is evident from fig. 4 a and b that T_g shifts to higher temperatures with increasing heating rate. The pronounced variation of T_g with heating rate is a manifestation of the kinetic nature of the glass transition which has been used to determine the activation energy of the transition from glassy to liquid state [25, 26, 39, 40]. There are several definitions for T_g included the extrapolated onset, the inflection point, the maximum point of the endothermic trace and the middle point of the endothermic trace which is employed in this work as seen in the fig.4 b. All of these definitions of T_g lead to the same result in calculation of the activation energy for different glasses.

It is well known that (T_g) of glassy alloys varies with the heating rate (ϕ) which follows empirical Lasocka's formula as [41]:

$$T_g = a + b \ln \phi \quad (9)$$

where a and b are constants for a given glass composition. As shown in Fig. 5 the plots of T_g against $\ln \phi$ describe the heating-rate dependence of T_g for 50TVK0, 50TVK5 and 50TVK10 samples. It is clear from this figure, the present data cannot be fitted to Eq. (9) for the whole range of ϕ and there are two different linear regions. Mehta et al. showed that the values of a and b are sensitive to the cooling rate of the melt which is related to the nature of the structural relaxation within the glass transition region [42]. It is evident from Fig. 5 that the values of a and b are different for different heating rate regions; these different values of a and b obtained in the present work may be related to a change in the transformation processes involved in the glass transition.

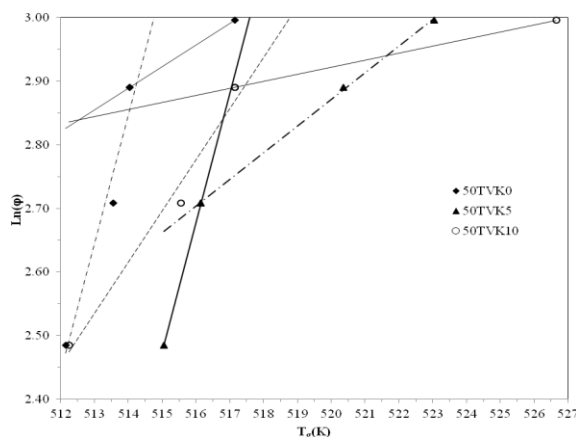


Fig. 5. Plots of T_g versus $\ln \phi$ for $50\text{TeO}_2-(50-x)\text{V}_2\text{O}_5-x\text{K}_2\text{O}$ ($x = 0, 5$ and 10) glasses. The solid and dashed lines represent fit to Eq. (9) at different heating rate regions

The heating and cooling rate dependence of the glass transition temperature has been studied widely based on the structural relaxation models [43-45]. Based on structural relaxation models, the heating and cooling rate dependence of the glass transition temperature was investigated by many authors [26, 33-36]. As presented in continuation, two frequently used equations for the structural relaxation are Moynihan and Kissinger [24-26]. In spite of the fact that Kissinger and Moynihan equations are basically and originally for the determination of the activation energy for the crystallization process, it has been shown that the same equations can be used for the evaluation of the activation energy of the glass transition process [46, 47] (to a high degree of approximation); conditions necessary for the validity of these equations are that the structural relaxation be describable by a temperature-independent distribution of relaxation times and that the glass be cooled from a starting temperature well above the transition region and subsequently reheated at the same rate starting from a temperature well below the transition region; therefore, it should be mentioned that the activation energies, calculated in this work, are of phenomenological effective values determined on the basis of Arrhenian activation process. Upon the above explanations, the model frequently used to determine the activation energy (ΔH^*) for structural relaxation in the glass transition region is given by Moynihan [25] as:

$$\ln\left(\frac{\phi}{T_g}\right) = \left(-\frac{\Delta H^*}{RT_g}\right) + C \quad (10)$$

where R is the gas constant and C is constant.

The value of ΔH^* is determined from the slope of the plots, $\ln \phi$ versus $1/T_g$.

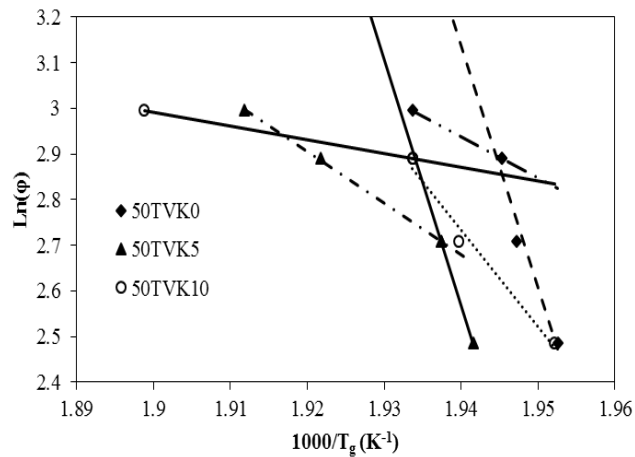


Fig. 6 Plots of $\text{Ln}(\varphi)$ versus $1000/T_g$ (Eq. 10) for 50TVKx glasses; straight lines are drawn for the guide for eye to distinct the different heating rate regions, and the slopes are equal to $(-\Delta H^*/1000 R)$

Based on another well-known approach, Kissinger model, the activation energy (ΔH^*) for structural relaxation in the glass transition region is expressed as:

$$\text{Ln}\left(\frac{\varphi}{T_g^2}\right) = \left(-\frac{\Delta H^*}{RT_g}\right) + C \quad (11)$$

where the gas constant and C is a constant.

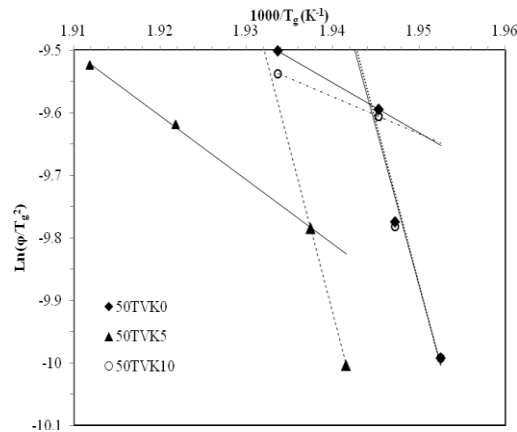


Fig. 6 Kissinger plots $\text{Ln}\left(\frac{\varphi}{T_g^2}\right)$ of versus $1000/T_g$ for 50TVKx glasses ($x = 0, 5$ and 10)

Thus, the slope of the $\text{Ln}(\varphi/T_g^2)$ vs. $1/T_g$ plot gives the value for ΔH^* . Both types of plots, $\text{Ln}(\varphi)$ vs. $1/T_g$ (Eq. (10)) and $\text{Ln}(\varphi/T_g^2)$ vs. $1/T_g$ (Eq. (11)), for the present glasses show, as expected, linear relationship with a linear correlation factor better than 0.9538. Such plots are shown in Fig. 5 and Fig. 6 for 50TVKx glasses. Furthermore, as is evident from Fig. 5 and Fig. 6, two regions can be identified in the plots. This leads to two different values for the activation energy in each heating rate region; the obtained data of ΔH^* are listed in table 2, for example in the case of 50TVK5 sample upon the Moynihan model (Eq. 10), in the low- φ region, the activation energy for the glass transition is 448.359 kJ/mole and in the high- φ region the activation energy is

93.881 kJ/mole; while, according to the Kissinger model (Eq. (11)), in the low- φ region, the activation energy for the glass transition is 439.807 kJ/mole and in the high- φ region the activation energy is 85.247 kJ/mole for the same sample. This deviation (existence of two φ -regions) from Moynihan or Kissinger et al. predictions shows that the glass transition process cannot be described by constant activation energy. It is worth mentioning that although Moynihan and Kissinger equations are based on different theoretical models, they both led to similar values of the activation energies in the lower and the higher heating rate regions, which suggest that both equations are useful in determining ΔH^* ; however, the ΔH^* values from Eq. (10), on the average, ~ 9 kJ/mol differ from those from Eq. (11). It should be mentioned here that the above analysis showed that even on the basis of Moynihan and Kissinger models, the process of glass transition cannot be described by single activation energy. Generally, it is believed [26, 29] that Moynihan and Kissinger equations are physically equivalent for the isokinetic processes and are valid only in narrow temperature ranges; therefore the obtained activation energies from these models are nearly the same. The role of shear modulus as an important thermodynamic and kinetic parameter governing the properties and relaxation of the glassy state has been emphasized; furthermore, in general, temperature dependence of shear modulus does not depend on heating rate at $T > T_g$; in other words, at $T < T_g$ shear viscosity depends on heating rate and is responsible for structural relaxation and related viscoelasticity [48]. Thus, it seems that the activation energies determined in the present work are the activation energy of the shear viscosity [26]. Similar behavior already has been observed in the ternary tellurite-vanadate glasses containing NiO [26] and Sb_2O_3 [29].

Based on table 2 and Fig. 7, the minimum value of ΔH^* between the present glasses is for 50TVK10, in both heating rate regions. This may be related to the concentration of non-bridging oxygens (NBOs) and the structural change in this system [26].

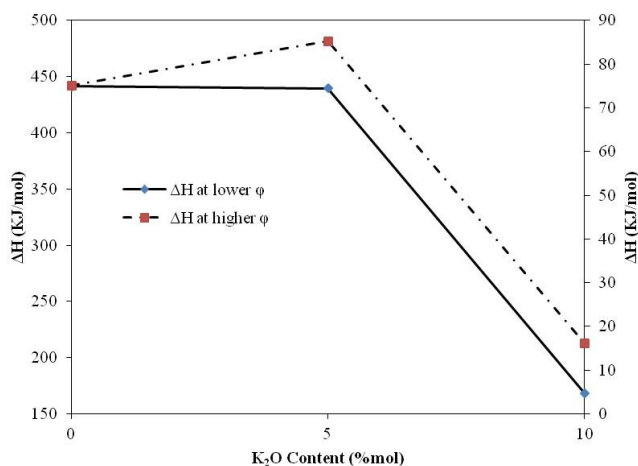


Fig. 7) Variation of ΔH^* against K_2O content (x) at different φ -regions obtained from Eq.10, for 50TVK x glasses

Table 2. Activation energy for glass transition ΔH^* determined using Kissinger equation at lower and higher heating rate regions, fragility (m) at lower heating rates and glass transition temperature (T_g) for 50TVKx glasses at the different heating rates (ϕ)

Glass	ϕ (K/min)	T_g (°C)	m	ΔH^* (kJ/mol) at lower	ΔH^* (kJ/mol) at higher
				ϕ	ϕ
50TVK0	12	239	44.19 (Eq.11)	432.810 (Eq.11) 441.362 (Eq.10)	66.545 (Eq.11) 75.122 (Eq.10)
	15	240.4			
	18	240.9			
	20	244			
50TVK5	12	241.9	45.65 (Eq.11)	439.807 (Eq.11) 448.359 (Eq.10)	85.247 (Eq.11) 93.881 (Eq.10)
	15	243			
	18	247.2			
	20	249.9			
50TVK10	12	239.1	17.58 (Eq.11)	168.533 (Eq.11) 177.097 (Eq.10)	16.137 (Eq.11) 25.114 (Eq.10)
	15	242.4			
	18	244			
	20	253.5			

On the other hand, the DSC data reported in table 2 show that for the different compositions at different heating rates, the glass transition temperature reaches to a peak in 50TVK5 and then decrease with the increasing potassium oxide content to 10% and all the other heating rates indicate similar behavior in exception with $\phi=20$ K/min for 50TVK10. The variation of T_g can be interpreted as a changing in the thermal stability of the glass. The thermal stability of the glass is a result of the glass structure; in other words, in this work, the change in T_g indicates a change related to the manner in which V_2O_5 and K_2O get arranged in the glass. This means that the glass-transition temperature varies with the average coordination number changes. This may be introduction of potassium oxide in high quantity causes a decrease in the number of V–O–V bonds and the increase of the V–O–K bonds. Moreover, it is known [49, 50] that TeO_4 triangular bipyramidal (tbp) units present in crystalline TeO_2 transform to TeO_3 triangular pyramids (tp) in some glasses. With the addition of K_2O in low and high content to 50TVKx systems, the transformation of tbps to tps and vice versa may occur which can be associated with changing in number of NBOs, providing effective impact in the weakness/strength character of the bonds in glass network.

One of the important parameters in amorphous materials is fragility, which was defined as the increasing rate of the viscosity of a supercooled liquid at the glass transition temperature during the process of cooling process [51]. The viscosity for strong glass-forming liquids follows Arrhenius temperature dependence with almost constant apparent activation energy for viscous flow. In contrast, the viscosity for fragile glass-forming liquids shows highly non-Arrhenius temperature dependence and exhibits steep changes in the apparent activation energy for viscous flow from a very low value above the melting temperature to a very high value when approaching the glass transition [52]. Fragility of a given glass can be quantified by the fragility index m which is a measure of the rate at which the relaxation time decreases with increasing temperature around T_g and is given by [53]:

$$m = \frac{\Delta H^*}{2.3RT_g} \quad (12)$$

where ΔH^* is the activation energy for glass transition in amorphous materials and R is gas constant. The fragility index values were calculated and listed in table 2 (see also fig. 8). The calculated m -values for 50TVKx glasses are in the range of 45.65–17.58. The upper and lower

limits of parameter m are theoretically estimated between 16 for ‘strong’ systems which are characterized by covalent directional bonds that form a spatial network and 200 for ‘fragile’ systems including molecular units connected by isotropic bonds of Van der Waals type [38]. The fragile structures are more susceptible to the thermal degradation in vicinity of the glass transition. It is clear from table 2 and fig. 8 that the value of m for 50TVK10 glassy alloy is near the lower limit ($m \approx 16$) which gives an indication that this prepared glass is obtained from strong glass forming liquids. In general, based on the m values listed in table 2, tellurite vanadate glasses containing potassium oxides can be considered in the strong glass category with high resistance against thermal shocks.

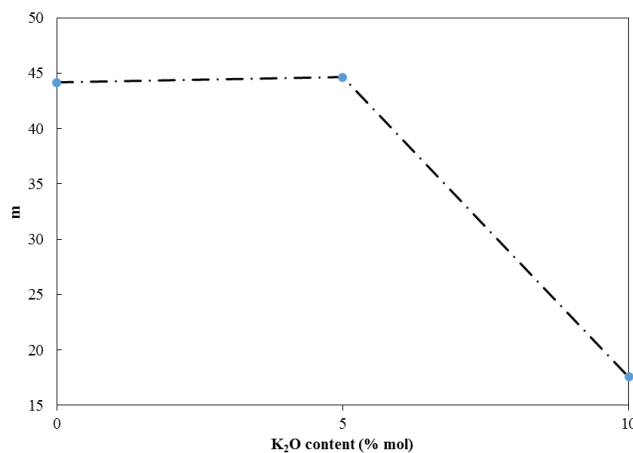


Fig. 8. The fragility parameter, m , for 50TVK0, 50TVK5 and 50TVK10 glasses

It has been shown [29] that the viscosity of a glass, η , at any temperature, T , near the glass transition region can be calculated with a reasonable accuracy from the glass transition temperature, T_g , and activation enthalpy for glass transition, ΔH^* , using the relation:

$$\text{Log}\eta(T) = 11.3 + (\Delta H^*/2.3R)[(1/T) - (1/T_g)] \quad (13)$$

The viscosity for the present tellurite glasses was calculated (Eq. 13) at a few selected temperatures above T_g and is shown as a function of temperature in Fig. 9.

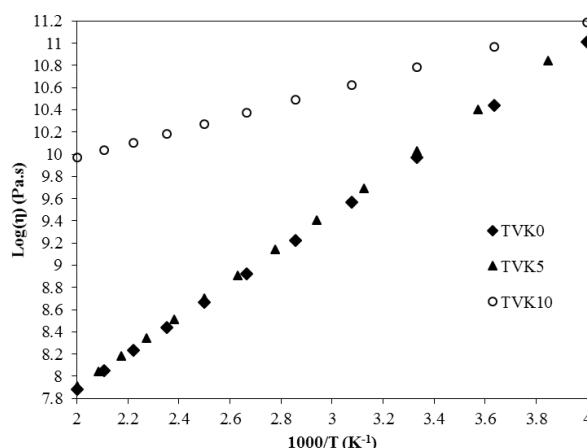


Fig. 9. Calculated viscosity as a function of $1000/T$ in the glass transition region for 50TVKx glasses (logarithmic function on the y-axis is in the base 10)

The value of T_g obtained from the DSC curve at a heating rate of 12 K/min for each glass was used in these calculations. As shown in Fig. 9, the viscosity at any given temperature for 50TVK10 is higher than two other sample which confirms lower m value for this sample as a

strong glass with high resistance against thermal shocks. There is no experimental data currently available for these glasses with which the calculated values of viscosity (Fig. 9) can be directly compared.

Furthermore, a relationship between kinetic fragility parameter m and mechanical properties has been established. It has been found that the fragility parameter has linear relation with the relative strength of K/S (K and S are bulk modulus and shear modulus, respectively) in different glasses [53, 54]. For present glasses, the relationship between kinetic fragility parameter and elastic modulus has been deduced by:

$$m = 311.46 \left[\left(\frac{K}{S} \right) - 1.94 \right] \quad (14)$$

The equation shows that there is correlation between the experimental data and theoretical results according to the Makishima and Mackenzie's hypothesis.

4. Conclusion

Investigation of elastic and thermal properties of $(50 - x)V_2O_5-50TeO_2-xK_2O$ glasses heating-prepared by melt quenching method has been investigated. It was observed that introduction of potassium oxide to oxide to tellurite - vanadate systems leads to decreasing in Shear, Bulk and Young's modulus for the understudied glasses. It was seen that there is a maxima in 50TVK5 sample Poisson ratio of the glasses which is similar with the observed behavior in glass transition temperature and density of 50TVKx compositions. Also, Investigation of heating-rate dependence of the glass transition temperature in the glasses was carried out using DSC technique in terms of Lasocka, Moynihan and Kissinger models. It was found that T_g shifted to higher temperatures with increasing of heating rates. It was shown in this study that the transition process cannot be described in terms of single activation energy, based on results derived from both Moynihan and Kissinger models. This study shows the assumption that the glass activation energy does not vary during the glass transition process is not valid. From the activation energy values, the fragility, m , was determined for the present glasses and was in range of 45.65–17.58. From the results it was indicated that 50TVK10 is the strongest glass composition between the prepared glasses. However, according to the fragility values, generally, 50TVKx glasses can be considered in the strong glass category with m value near to 16. The calculated viscosity values in function of temperature confirmed the obtained data from measuring the fragility. The relationship between kinetic fragility parameter m and elastic modulus was established, showing logical correlation between the experimental calorimetric data and theoretical results based on the Makishima and Mackenzie's model.

References

- [1] B. Oz, M.L. Ovecoglu, I. Kabalci, G. Ozen *J Eur Ceram Soc* **27**, 3239 (2007)
- [2] R Stepiena, R Buczynski, D Pysz, I Kujawa, et al, *J Non Cryst Solids* **357**(3), 873 (2011).
- [3] G Turkey, M Dawy, *Mater Chem Phys* **77**, 48 (2003)
- [4] D. Souri, *J Non Cryst Solids* **356**, 2181 (2010)
- [5] D Souri, SA Salehizadeh, *J Mater Sci* **44**(21), 5800 (2009)
- [6] D Souri, K Shomalian, *J Non Cryst Solids* **355**, 1597 (2009)
- [7] R El-Mallawany, MD Abdalla, IA Ahmed, *Mater Chem Phys* **109**, 291 (2008)
- [8] P Mosner, K Vosejpkova, L Koudelka, L Benes, *J Therm Anal Calorim* **107**(3), 1129 (2012)
- [9] GS Murugan, Y Ohishi, *J Non Cryst Solids* **341**, 86 (2004)
- [10] K Sega, Y Kuroda, H Sakata, *J Mater Sci* **33**, 1303 (1998)
- [11] T Kosuge, Y Benino, V Dimitrov, R Sato, T Komatsu, *J NonCrys Solids* **242** 154 (1998)

- [12] D Munoz-Martín, MA Villegas, J Gonzalo, JM Fernández-Navarro, *J Eur Cer Soci* **29**, 2903 (2009)
- [13] M Çelikbilek, AE Ersundu, S Aydin, *J Non Cryst Solids* **378**, 247 (2013)
- [14] EF Lambson, GA Saunders, B. Bridge, El-Mallawany RA, *J Non Cryst Solids* **69**, 117 (1984)
- [15] P Rozier, A Burian, GJ Cuello, *J Eur Cer Soci* **31**(15), 2775 (2011)
- [16] D Souri, M Elahi, *Phys Scr* **75**, 219 (2007)
- [17] RP Sreekanth Chakradhar, KP Ramesh, JL Rao, J Ramakrishna, *J Non Cryst Solids* **351**, 1289 (2005)
- [18] MA Sidkey, MS Gaafar *Ultrasonic Phys B: Cond Mat* **348**(1–4):46 (2004).
- [19] G Yankov, L Dimowa, N Petrova, M Tarassov et al *Opti Mater* **35**(2), 248 (2012)
- [20] D Zhu, CS Ray, W Zhou, DE Day, *J Non Cryst Solids* **319**, 247 (2003)
- [21] MP Kumar, T Sankarappa, AM Awasthi, *Physica B* **403**, 4088 (2008)
- [22] K Sega, Y Kuroda, H Sakata, *J Mater Sci* **33**, 1303 (1998).
- [23] R El-Mallawany, A Abousehly, E Yousef, *J Mater Sci Lett* **19**, 409 (2000)
- [24] D Souri, SA Salehizadeh, *J Ther Anal Calor* **112**(2), 689 (2012)
- [25] D Souri *J Mater Sci* **46**(21), 6998 (2011)
- [26] SA Salehizadeh, D Souri *J Phys Chems Solids* **72**(11), 1381 (2011)
- [27] D Souri Fragility, DSC and elastic moduli studies on tellurite–vanadate glasses containing molybdenum Measurement **44**(10), 1904. (2011)
- [28] D. Souri, *Eur Phys J B* **84**, 47 (2011).
- [29] D. Souri *J. Mater. Sci* **47**(2), 625 (2012).
- [30] M Farahmandjou, SA Salehizadeh, *Glass Phys Chem* **39**(5), 473 (2013)
- [31] A Makishima, JD Makenzie *J Non Cryst Solids* **12**, 147 (1975)
- [32] DR Lide *CRC handbook of chemistry and physics* 88th edition Boca Raton: CRC press. (2008)
- [33] S Inaba, S Oda, K Morigani, *J Non Cryst Solids* **325**, 258 (2003)
- [34] E Duval, T Deschamps, L Saviot, *J Chemi Phys* **139**, 064506 (2013)
- [35] R El-Mallawany, A Abousehly, E Yousef, *J Mater Sci Lett* **19**(5), 409 (2000).
- [36] Y Dimitriev, V Dimitrov, M Arnaudov, D Topalov, *J NonCryst Solids* **57**, 147 (1983)
- [37] BI Sharma, PS Robi, A Srinivasan, *s Mater Lett* **57**, 3504 (2003)
- [38] OA Lafi, MMA Imran, *J Alloy Comp* **509**(16), 5090 (2011)
- [39] S Kumar, K Singh *Thermochi Acta* **528**, 32 (2012)
- [40] S Vyazovkin, N Sbirrazzuoli, I Dranca *Rapid Commun* **25**(19), 1708 (2004)
- [41] M Lasocka *Mater Sci Eng* **23**(2–3), 173 (1976).
- [42] N Mehta, RK Shukla, A Kumar, *Chalcogenide Lett* **1**(10), 131 (2004)
- [43] H Ritland, *J Am Ceram Soc* **39**(12), 403(1956).
- [44] I Avramov, *Thermochim Acta* **280-281**, 363 (1996).
- [45] I Avramov, N Avramova *J Non Cryst Solids* **260**(1–2), 15 (1999)
- [46] JE Shelby, *J Non Cryst. Solids* **34**(1), 111 (1979)
- [47] J Colmenero, JM Barandiaràn, *J Non Cryst Solids* **30**(3), 263 (1979)
- [48] YP Mitrofanov, VA Khonik, AV Granato, DM Joncich, SV Khonik, *J Appl Phys* **109**, 073518 (2011)
- [49] T Komatsu, T Noguchi, R Sato, *J Am Ceram Soc* **80**(6), 1327 (1997).
- [50] T Komatsu, T Noguchi, Y Benino *J Non Cryst Solids* **222**, 206 (1997)
- [51] CA Angell *Science* **267**, 1924. (1995)
- [52] GJ Fan, H Choo, PK Liaw *J NonCryst. Solids* **351**(52–54), 3879 (2005)
- [53] ES Park, JH Na, DH Kim *Appl Phys Lett* **91**, 031907 (2007)
- [54] WH Wang, *J Appl Phys* **99**, 093506 (2006)